

Predictive Traffic Rule Compliance using Reinforcement Learning

Yanliang Huang, Sebastian Mair, Zhuoqi Zeng, Amr Alanwar, Matthias Althoff

Abstract—Autonomous vehicle path planning has reached a stage where safety and regulatory compliance are crucial. This paper presents a new approach that integrates a motion planner with a deep reinforcement learning model to predict potential traffic rule violations. In this setup, the predictions of the critic directly affect the cost function of the motion planner, guiding the choices of the trajectory. We incorporate key interstate rules from the German Road Traffic Regulation into a rule book and use a graph-based state representation to handle complex traffic information. Our main innovation is replacing the standard actor network in an actor-critic setup with a motion planning module, which ensures both predictable trajectory generation and prevention of long-term rule violations. Experiments on an open German highway dataset show that the model can predict and prevent traffic rule violations beyond the planning horizon, significantly increasing safety in challenging traffic conditions.

Index Terms—Autonomous driving, reinforcement learning, traffic rule compliance

I. INTRODUCTION

THE field of autonomous driving has advanced substantially over the past five years. Although perception and prediction modules have become more reliable, planning systems still face challenges, particularly regarding safety assurance and operational robustness. Furthermore, traffic rule compliance remains a fundamental prerequisite for autonomous vehicles, both to protect road users and to satisfy legal certification standards.

Recent research has effectively applied temporal logic to formalize traffic rules, enabling automated online monitoring systems [10], [11], [14] to continuously monitor the compliance of traffic rules. This approach uses the concept of rule robustness—a quantitative metric indicating how thoroughly specific traffic rules are satisfied or violated. Integrating such monitors into autonomous driving frameworks can help prevent rule violations within the planning horizon.

However, a significant challenge emerges from the limited prediction horizons of autonomous driving modules, particularly in complex traffic scenarios. Current planning strategies, which respond solely to immediate violations, are unable to anticipate potential infringements beyond their present scope. This limitation underscores the critical need to extend rule compliance prediction beyond the immediate horizon, especially for rules involving multi-object interactions and highly susceptible to abrupt environmental changes.

Building on steady progress in machine learning, there has been remarkable success in various autonomous driving applications, particularly in the interpretation of intricate

traffic patterns and prediction of vehicle behaviors [7]. In addition, reinforcement learning (RL) is especially suited for autonomous driving tasks due to its ability to adapt to complex environments, continuously learn and improve, and integrate rules with learning.

Building on these foundations, we propose a new actor-critic-style deep reinforcement learning (DRL) framework that incorporates a hierarchically structured rule book comprising German interstate traffic rules. To facilitate predictive traffic rule compliance, we use the temporal logic robustness of these rules as reward signals, enabling the critic network to learn state-value functions that indicate potential rule violations. The learned value function then guides the actor’s exploration.

Despite the benefits of DRL, agents often struggle with convergence in complex motion planning tasks involving multiple constraints. Although certain methods aim to enhance RL training efficiency [15], the outputs of actor networks can remain unstable, which requires extensive training for satisfactory performance.

To overcome these limitations, we propose a hybrid approach: instead of depending exclusively on DRL for exploration, we incorporate a motion planner as the actor component. In this thesis, we adopt the Commonroad Reactive Planner [21], which has demonstrated both efficiency and reliability in generating robust, explainable trajectories. This planner leverages a lattice-based methodology [19], [20] to produce candidate trajectories and identifies the optimal path via a cost function.

In a conventional actor-critic (AC) approach, critic evaluation provides feedback to the actor (policy network), guiding policy improvements. To integrate an actor-critic framework into our system, we embed the critic’s output directly into the motion planner’s cost function, thus selecting trajectories based on predicted state values. In other words, the planner prefers routes with higher state values, which are more likely to avoid long-term traffic rule violations. This method effectively mirrors on-policy learning by synchronizing the actor’s decisions with updates to the critic network during exploration.

During inference, the motion planner reuses state-value estimates and incorporates additional cost factors to balance comfort, safety, and goal reachability, thereby enabling flexible configuration.

Recognizing the importance of high-quality representations of environmental states in reinforcement learning, we employ a Graph Neural Network (GNN) architecture [13] as a feature extractor. This framework captures arbitrary road layouts and varying numbers of surrounding vehicles, while allowing flexible choices of input features. As a result, our agent benefits

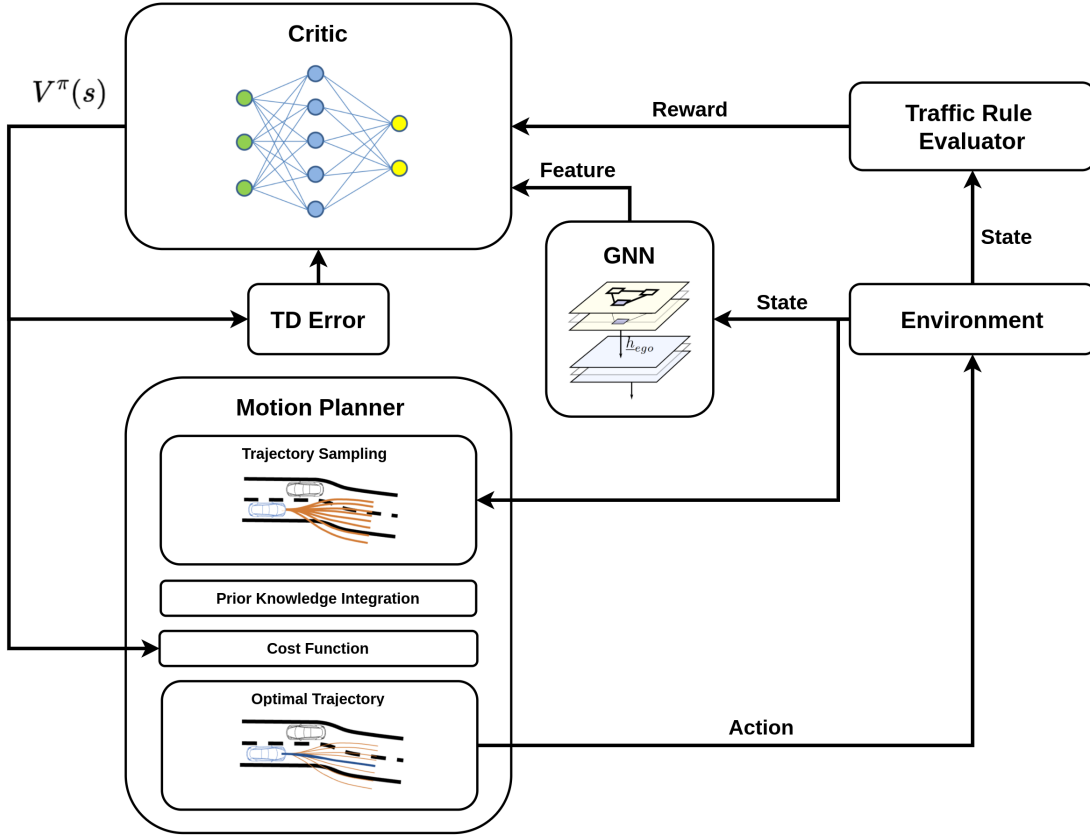


Fig. 1. Overview of our proposed framework for traffic rule-aware motion planning.

from a comprehensive state representation. An overview of the proposed approach is presented in Figure 1.

In this paper, we present a new approach for predicting future traffic rule violations by integrating reinforcement learning with lattice-based motion planning. Our work makes several key contributions to the field of autonomous driving:

- 1) We select three German interstate traffic rules that emphasize the importance of predictive traffic rule compliance.
- 2) We design a plug-and-play modular predictive traffic rule compliance system that can be integrated with an existing autonomous driving motion planner.
- 3) We pioneer the integration of actor-critic reinforcement learning with planning methods, creating a framework that combines the strengths of both.
- 4) We use a graph-based model to efficiently extract and process complex traffic data, allowing robust feature representation.
- 5) We validate our approach through extensive experiments on real-world traffic data, demonstrating its practical applicability and effectiveness.

To the best of our knowledge, this is the first successful integration of actor-critic reinforcement learning algorithms with cost-based motion planning in autonomous driving. Our work opens new avenues for uniting learning-based prediction with explainable planning methods, particularly for forecasting and preventing future traffic rule violations.

II. BACKGROUND

A. Reinforcement Learning

Reinforcement learning (RL) is a powerful machine learning paradigm that enables an agent to learn optimal decision-making strategies by interacting with an environment to maximize a cumulative reward signal. Unlike supervised learning, which depends on large, pre-labeled datasets, RL adopts a trial-and-error approach, allowing the agent to mirror natural learning processes through direct environmental feedback. This framework is particularly well suited for solving Markov Decision Processes (MDPs), which formalize the environment in terms of states $s \in \mathcal{S}$, actions $a \in \mathcal{A}$, transition probabilities $P(s'|s, a)$, and rewards $r(s, a, s')$. The agent's goal is to derive a policy - a mapping from states to actions $\pi : \mathcal{S} \rightarrow \mathcal{A}$ - that optimizes the expected long-term reward [17].

To evaluate the quality of states and pairs of state actions, RL algorithms define value functions. The state value function $V^\pi(s)$ represents the expected return of the state s following policy π :

$$V^\pi(s) = \mathbb{E}_\pi[G_t | S_t = s] \quad (1)$$

One way to solve MDPs with RL is the actor-critic method. It consists of two complementary components:

- Actor: Develops a policy $\pi(s)$ that generates actions, typically using a stochastic policy with a distributional output layer.

- Critic: Evaluates the quality of states through a value function $V(s)$, where s denotes the system state [17].

In standard implementations, the actor approximates the policy $\pi_\phi(a|s)$ and the critic approximates the state-value function $V_\xi(s)$, both using multilayer perceptrons (MLPs). These components maintain separate training processes but are updated simultaneously. The critic typically learns state values through methods like temporal difference (TD) learning or Monte Carlo estimation, providing feedback to refine the actor’s policy.

Despite its promise, applying DRL to autonomous driving introduces challenges. The high-dimensional state spaces, multi-agent interactions, and the need to embed traffic rules and safety constraints into the learning process require tailored algorithmic advancements.

B. Graph Representation and Graph Neural Network

Graphs offer a powerful framework for modeling complex systems by representing entities as nodes and their relationships as edges. This structure excels at capturing topological relationships and dynamic interactions, making it particularly valuable in traffic scenarios where vehicles, pedestrians, and infrastructure elements interact. The graph is formally defined as $G = \{N, E\}$, where $N = \{n_i, i \in \{1, 2, \dots, n\}\}$ represents the set of node attributes and $E = \{e_{ij}, i, j \in \{1, 2, \dots, n\}\}$ denotes the set of edge attributes; n represents the total number of vehicles in the constructed graph [4].

GNNs offer a framework for modeling the intricate relationships present in traffic environments, particularly the complex structures of the road network and dynamic vehicle interactions. Their effectiveness comes from the introduction of a relational bias to the learning problem through explicit modeling of connections between objects in the graph structure [4].

C. Traffic Rules Formalization

Formalizing traffic rules into quantifiable metrics poses a significant hurdle for RL agents. Simple rules, such as speed limits, can be encoded directly through violation penalties, for example, a negative reward for exceeding a threshold. However, more sophisticated rules, such as *“the ego vehicle must maintain sufficient speed to avoid impeding traffic flow,”* require comprehensive contextual information and cannot be adequately captured by binary compliance (satisfied or violated). Real-world driving often involves continuous degrees of adherence to the rules, and Boolean representations do not account for reasonable deviations, such as temporarily exceeding a speed limit to avoid an obstacle.

To overcome these limitations, formal temporal logic frameworks have emerged as powerful tools for specifying and evaluating traffic rules. Linear Temporal Logic (LTL) has been used to formulate traffic rules in an automatically evaluable syntax [3], [16]. However, its discrete-time framework limits its suitability for online evaluation in RL, where real-time adaptability is essential. Signal Temporal Logic (STL), as an extension of Metric Temporal Logic (MTL) [8], addresses

these shortcomings by specifying properties of continuous-time signals [12]. Unlike MTL’s Boolean satisfaction values, STL introduces quantitative semantics through the degree of robustness, which measures the degree of satisfaction or violation of the rule [5]. This makes STL ideal for autonomous driving, where compliance often exists on a spectrum.

III. METHODOLOGY

In this section, we introduce our proposed method for predicting and preventing future traffic rule violations in autonomous driving scenarios. Our approach integrates a modified RL framework with a motion planner, leveraging the complementary strengths of both techniques to ensure that traffic rule compliance extends beyond the immediate planning horizon.

Our method employs a Graph Neural Network (GNN) extractor within an actor-critic RL framework, coupled with a motion planner, to train an ego agent to navigate highway scenarios while adhering to hierarchical traffic rules. Specifically, we focus on trucks operating on German interstate highways, where scenarios involve multiple lanes and traffic participants.

Unlike many existing approaches that rely on simulators to model the motion of traffic participants, we utilize a series of recorded scenarios for training instead of interactive scenarios. This choice is intentional: In reactive simulations, other vehicles actively avoid the ego vehicle, potentially simplifying the learning task and leading to overly aggressive or less robust agent behavior. In contrast, recorded scenarios present static, unresponsive traffic participants, creating more challenging conditions that rigorously test the ego agent’s planning and obstacle avoidance capabilities.

The primary objective of our algorithm is to enable the ego vehicle to achieve multiple goals. First, the agent derives a state value from the input features of the current scenario, obtained through sensors and other data sources, that represents the long-term cumulative reward associated with compliance with specific traffic rules. Then, by selecting the trajectory with the highest state value, the ego vehicle leverages the motion planner to generate a path that predictively prevents long-term rule violations.

To enhance this process, we integrate traffic rules with varying weights based on their hierarchical importance, as defined by a rule book. In addition, we incorporate cost functions to ensure that planned trajectories are goal-oriented, safe, and comfortable. Through this comprehensive approach, our goal is to develop a robust planner that delivers exceptional performance in complex driving environments.

A. Selection and Formulation of Traffic Rules

This study centers on autonomous driving scenarios along the German interstate system, extending the foundational research presented in [11]. In that work, seven interstate traffic rules were formalized using Signal Temporal Logic (STL), drawing from the German Road Traffic Regulation (StVO), the Vienna Convention on Road Traffic (VCoRT), and legal expertise. These rules address critical aspects of driving, including safety, speed limits, traffic flow, and local

customs. However, not all of these formalized rules pose significant challenges or are equally relevant to our proposed methodology.

For instance, Rule R_{G3} , which governs speed limits, can be incorporated into a motion planner through straightforward techniques. This can be achieved either by integrating a simple cost function that penalizes trajectories exceeding the speed limit or by filtering out non-compliant routes entirely. Similarly, Rule R_{G2} proves relatively trivial to enforce within our framework. Compliance can be ensured by evaluating the robustness of this rule across sampled trajectories within the planning horizon and selecting the optimal trajectory accordingly. Given the ease of adherence, violations of R_{G2} are infrequent and can be readily avoided using conventional planning methods.

Consequently, our approach emphasizes scenarios where conventional rule-encoding strategies are inadequate, highlighting the advantages of our data-driven, neural network-based methodology. For example, a vehicle with a 2 seconds prediction and planning horizon cannot effectively handle a rule violation at 2.1 seconds, since its motion planning and control systems typically cannot adjust in time, inevitably leading to a rule violation. To this end, we have carefully selected two representative rules from [11] that pose more complex challenges, requiring a sophisticated integration of traffic regulations into the autonomous vehicle decision-making process. Furthermore, we introduce a newly formalized rule to underscore the critical role of our method in addressing intricate traffic scenarios. This selection and formulation highlight the shortcomings of traditional approaches and illustrate the potential of our advanced techniques to improve autonomous driving performance on German interstates.

The rules are as follows:

- **R_{G1} - Safe distance to preceding vehicle:** The ego vehicle following vehicles within the same lane must maintain a safe distance to ensure collision freedom, even if one or several vehicles suddenly stop. If another vehicle causes a safe distance violation due to a cut-in maneuver, the ego vehicle must recover the safe distance within a predefined time t_c after the start of the cut-in [11].
- **R_{I2} - Driving faster than left traffic:** The ego vehicle is not allowed to drive faster than any vehicle in the lanes to the left of it. Exception is the vehicle in the left lane is part of a queue of vehicles, slow-moving traffic, or congestion and the ego vehicle drives with only slightly higher speed [11].
- **R_{I6} - No overtaking sign:** When the ego vehicle encounters a no overtaking sign, it must remain in the rightmost lane.

The detailed formulas for these rules, formalized using Signal Temporal Logic (STL), are presented in Table I.

We select rule R_{G1} , the safe distance rule, as the initial test of the validity of our approach. For a motion planner, compliance with this rule is generally straightforward, with robustness cost in trajectory selection sufficing in most cases. However, when a preceding vehicle brakes abruptly due to congested traffic, the planner may fail to respond quickly enough, resulting in a violation. In contrast, our RL-based

method leverages a comprehensive view of the scenario within the sensor range to predict other agents' braking, enabling proactive decision-making to maintain a safe distance.

Furthermore, we simplified rule R_{I2} , omitting certain exception conditions present in [11], as our dataset lacks broad lane markings and ramps, but the simplified rule retains its relevance. Our RL method may outperform approaches that rely solely on the cost of robustness, particularly when a slow-moving vehicle in the left lane exhibits a significant velocity difference relative to the ego vehicle. In such cases, a predictive approach can exploit additional information to initiate maneuvers earlier.

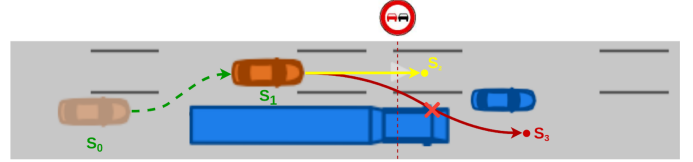


Fig. 2. A scenario where predictive methods are needed

Beyond the rules adopted directly from [11], we formalize a new rule, R_{I6} , based on German traffic regulations. According to §2(1) of the StVO, on multi-lane roadways in one direction, vehicles may deviate from the obligation to drive as far right as possible. Section §5(1) mandates overtaking on the left lane, while §5(3) prohibits overtaking when indicated by traffic signs (e.g., Sign 276 or 277). Thus, for maximum compliance, a vehicle should remain in the rightmost lane when passing a *no overtaking* sign. Although simple, this rule presents challenges in specific scenarios.

Consider, for example, a situation where an ego vehicle is overtaking a long truck on a two-lane road. A planning method based solely on robustness cost would maintain compliance with R_{I6} until the vehicle is near the traffic sign. However, as the vehicle approaches the sign, there may be insufficient time and space to complete the overtaking maneuver or safely return to the right lane. As illustrated in Figure 2, the green arrow represents a rule-compliant trajectory, the yellow arrow indicates a rule-violated trajectory, and the red arrow denotes an infeasible trajectory. Within its immediate planning horizon, the ego vehicle can maintain compliance with traffic rules. However, it is unable to reposition itself into the right lane before encountering the *no overtaking* sign. This constraint inevitably leads to a rule violation, exposing a key limitation of traditional planning approaches: breaches may become unavoidable when the planning horizon fails to anticipate downstream constraints.

In contrast, a predictive approach offers a robust solution. By detecting the *no overtaking* sign within the vehicle sensor range, the system can preemptively maneuver to the right lane well before reaching the prohibited zone. This strategy prevents further overtaking attempts as the vehicle approaches the sign, ensuring full compliance with R_{I6} .

To address potential rule conflicts, we implemented a hierarchical rule book structure [2] that reflects the natural priority ordering of traffic rules. This structure acknowledges that lower-priority rules may need to be temporarily violated to

TABLE I
OVERVIEW OF FORMALIZED TRAFFIC RULES.

Rule	Law reference	STL formula
R_G1	§4(1) StVO; §13(5) VCoRT	$G(\text{in_same_lane}(x_{\text{ego}}, x_0) \wedge \text{in_front_of}(x_{\text{ego}}, x_0) \wedge \neg \mathbf{O}_{[t, t_c]}(\text{cut_in}(x_0, x_{\text{ego}})) \wedge \mathbf{P}(\neg \text{cut_in}(x_0, x_{\text{ego}}))) \Rightarrow \text{keeps_safe_distance_prec}(x_{\text{ego}}, x_0)$
R_I2	§7(2), §7(2a), §7a StVO; [1] StVO §5 Rn. 58, [1] StVO §18 Rn. 10-11	$G(\forall x_0 : \text{left_of_i}(x_0, x_{\text{ego}}) \wedge \text{drives_faster_i}(x_{\text{ego}}, x_0) \Rightarrow (\text{in_congestion}(x_0) \vee \text{in_slow_moving_traffic}(x_0) \vee \text{in_queue_of_vehicles}(x_0)))$
R_I6	§2(1), §5(1)(3) StVO; traffic sign 276	$G(\text{no_overtaking_sign}(x_{\text{ego}}) \rightarrow \text{in_rightmost_lane}(x_{\text{ego}}))$

satisfy higher-priority rules in challenging situations. R_{G1} receives highest priority due to its direct impact on collision avoidance and safety-critical interactions. R_{I6} follows as the second-highest priority due to its role in maintaining traffic order and preventing dangerous overtaking behaviors. R_{I2} receives the lowest priority as it primarily affects traffic efficiency rather than immediate safety concerns. Following this prioritization, we establish the rule book hierarchy:

$$R_{G1} > R_{I6} > R_{I2}$$

B. Graph Representation and GNN

In this section, we introduce the method used to embed traffic scenario input features into a meaningful representation using Graph Neural Networks (GNNs).

To begin, we construct a graph representation of the traffic scenario. A graph consists of nodes and edges. In the context of traffic, the nodes could represent vehicles, lanes, or other participants such as bicycles and pedestrians. However, given the location on the highway, we exclude non-vehicle participants. Furthermore, the relatively simple layout of the lane of the roads, mainly consisting of roads and ramps, makes the use of lanelets unnecessary. Representing lanelets as nodes would introduce multiple node types, resulting in a heterogeneous graph, which is more complex to process with GNNs. Consequently, we simplify the representation by using only vehicle nodes connected by vehicle-to-vehicle (V2V) edges to form the graph.

In the work by [6], the V2V graph is constructed using basic kinematic vehicle features and relative position edge features, as detailed in Table II. However, these features alone are insufficient for the model to develop a comprehensive understanding required to predict the compliance with traffic rules. To address this limitation, we enhance the graph representation by incorporating additional features designed to help the model recognize specific patterns associated with rule compliance.

Drawing inspiration from [15], who employ rule robustness as node features and predicates such as *CutIn* and *InFrontOf* as edge features, we initially considered a similar approach. However, the computational overhead of repeatedly extracting features and calculating robustness proved prohibitive for our method, which involves numerous iterative operations. Instead,

TABLE II
GRAPH FEATURE DEFINITIONS

Feature	Ego Feature name	Normalization function
<i>Existing vehicle node features</i>		
$f_{p,x}$	PosEgoFrameX	$f_{p,x}/50$
$f_{p,y}$	PosEgoFrameY	$f_{p,y}/50$
f_v	Velocity	$(f_v - 15)/20$
<i>Existing ego vehicle features</i>		
f_a	Acceleration	$f_a/20$
f_v	Velocity	$(f_v - 15)/20$
f_y	YawRate	$\min(\max(f_y, -1), 1)$
<i>Existing Vehicle-to-vehicle edge features</i>		
$f_{rp,x}$	RelativePosEgoX	$f_{rp,x}/50$
$f_{rp,y}$	RelativePosEgoY	$f_{rp,y}/50$
<i>Added vehicle node features</i>		
$f_{l,L}$	Lane	$f_{l,L}$
<i>Added ego vehicle features</i>		
$f_{lb,L}$	DistLeftBound	$f_{lb,L}/2$
$f_{rb,L}$	DistRightBound	$f_{rb,L}/2$
$f_{lrb,L}$	DistLeftRoadBound	$(f_{lrb,L} + f_{lb,L})/12$
$f_{rrb,L}$	DistRightRoadBound	$(f_{rrb,L} + f_{rb,L})/12$
$f_{h,L}$	HeadingError	$\min(\max(f_{h,L}, -\pi/4), \pi/4)$
$f_{la,L}$	GoalDistLateral	$\log(f_{la,L} + 1) f_{la,L} / f_{la,L} $
$f_{lo,L}$	GoalDistLongitudinal	$\log(f_{lo,L} + 1) f_{lo,L} / f_{lo,L} $
$f_{l,L}$	Lane	$f_{l,L}$
$f_{nots,L}$	NonOvertakingTSRelative	$(f_{nots,L} - 50)/50.0$
<i>Added Vehicle-to-vehicle edge features</i>		
$f_{rv,x}$	RelativeVelocityEgoX	$f_{rv,x}/20.0$
$f_{rv,y}$	RelativeVelocityEgoY	$f_{rv,y}/20.0$
$f_{lo,LT}$	LeftOf	$f_{lo,LT}$
$f_{sl,LT}$	SameLane	$f_{sl,LT}$

we adopt simpler, yet targeted, features tailored to our specific traffic rules. The enhanced graph representation, including these additional features, is also presented in Table II.

Intuitively, the ego vehicle has access to more detailed information than other agents. Therefore, in addition to standard node and edge features, we incorporate extensive ego-specific features, which are later combined with the embedded features from the GNN. Key additions include features such as *DistLeftBound*, *DistRightBound*, *DistLeftRoadBound*, and *DistRightRoadBound*, which are added to both vehicle and ego features to enable vehicles to localize themselves within the lanelet network. Since lanelets are not represented as nodes, these features are essential for recognizing lane-related rules, all of which are relevant to our selected rules. Additionally, a *Lane Feature* explicitly indicates the lane occupied by each vehicle, facilitating the assessment of rule compliance. For traffic rule R_{I6} , we introduce the *NonOvertakingTSRelative*

feature, which provides the relative longitudinal distance to the next “no overtaking” traffic sign, based on a sensor radius of 100 meters. This range ensures the vehicle has sufficient time to maneuver and avoid violations. The distance resets to the next relevant sign upon encountering a “no overtaking end” sign. Furthermore, *HeadingError* and goal-related features enhance the ego vehicle’s situational awareness and support goal-oriented planning.

For V2V edge features, we introduce the *RelativeVelocity* feature, which is critical for ensuring the ego vehicle does not exceed the speed of the vehicle to its left, supporting compliance with rule R_{I2} . The *LeftOf* feature mimics the predicate calculation for “LeftOf,” providing expressive information with low computational complexity. Additionally, the *SameLane* feature aids in understanding rule R_{G2} , which relates to interactions with vehicles in the same lane.

By integrating these features, we provide the model with rich, context-aware information to enable accurate predictions of traffic rule compliance.

C. Modified Actor-Critic Algorithm

The actor-critic method is a widely recognized approach in deep reinforcement learning (DRL). In this framework, the critic learns a value function that guides the actor’s policy optimization. During training, these two networks are deeply interdependent: the critic’s value estimates shape the actor’s policy updates, while the actor’s actions generate new experiences that refine the critic’s value assessments. This mutual learning process typically drives both networks toward optimal behavior.

However, applying this method to autonomous driving presents significant challenges. When a neural network serves as the actor, its black-box nature raises concerns about interpretability and controllability. Integrating prior knowledge, such as traffic rules, becomes difficult, potentially leading to unsafe or unstable vehicle behaviors that are difficult to debug or constrain. Furthermore, a randomly initialized neural network actor begins by making random decisions, which impedes effective exploration. This issue is particularly pronounced in interstate traffic scenarios, where the navigable space is narrow relative to the length of the route. Random actions often result in off-road terminations, preventing the agent from reaching its goal.

To address these limitations, we propose replacing the traditional actor network with a motion planner equipped with a cost function. This planner incorporates critical prior knowledge on trajectory feasibility and safety, including kinematic constraints. Ensures physically feasible trajectories by verifying the kinematic feasibility and collision avoidance before selecting the optimal trajectory based on a predefined cost function. Unlike a neural network, the planner’s decision-making process is interpretable and adjustable. By integrating a series of modules, we can embed prior knowledge into the planner, enabling it to explore the environment more effectively across diverse scenarios.

The effectiveness of this replacement stems from the fact that the output of the value network approximates the state

value, which represents the cumulative rewards following the policy. When using robustness of traffic rules as a reward, a higher state value indicates that the vehicle is more likely to comply with rules in that state, while a lower value suggests the opposite. This information is essential to avoid long-term violations of traffic rules. Consequently, in the training phase of our approach, the motion planner selects trajectories using a state-value-guided mechanism.

Let $V^*(s)$ represent the output of the well-trained value function for a state s , and let $\tau_1, \tau_2, \dots, \tau_n$ denote the set of candidate trajectories generated by the planner. Each trajectory τ_i is a sequence of collision-free and kinematically feasible states, verified by a previously implemented checker. We define the cost for each trajectory τ_i as follows:

$$C(\tau_i) = \sum_{s_{ij} \in \tau_i} (-w_{ij} * V^*(s_{ij})), \quad (2)$$

where w_{ij} are the weighting factors assigned to each state. The optimal trajectory is selected as:

$$\tau^* = \arg \min_{\tau_i} C(\tau_i). \quad (3)$$

This selection process identifies a macro-action, a trajectory spanning multiple time steps that balances long-term value with prior knowledge. The motion planner constrains the action space to a finite set of trajectories satisfying kinematic and safety requirements. By incorporating $-V^*(s_{ij})$ into the cost function, an estimate of future returns is included for each state s_{ij} along the trajectory τ_i . The critic then updates its value network based on rollouts collected through the actor’s exploration. This approach aligns with the actor-critic framework’s core principle: the actor selects actions according to the current policy, the critic evaluates the outcomes and estimates their quality, and the actor refines its policy using the critic’s feedback.

During the exploration phase, rather than employing a ϵ -greedy strategy, a greedy strategy is adopted with random start and goal settings and a planned route. Since the motion planner generates trajectories around the route, randomly created routes ensure comprehensive coverage of all possible states. Furthermore, given the relatively straightforward nature of interstate scenarios, this greedy strategy suffices to encompass nearly all potential situations.

After each exploration step, rule-specific robustness rewards are computed for every state. The training procedure alternates between the exploration and update phases, collecting rollouts prior to updating the network. The critic network is trained to minimize the temporal difference (TD) error.

Due to the real-time updates of both the actor and critic, and since the critic’s state value updates depend on the next states produced by the current policy, this method achieves on-policy learning while maintaining high sample efficiency.

Our method offers significant flexibility. In conventional RL approaches, it is necessary to integrate all rewards that represent multiple planning goals. This often creates challenges when attempting to incorporate new planning goals or constraints, as it typically requires retraining the model from scratch.

In contrast, our approach allows a trained critic to represent the state-value for one or multiple rewards, enabling the combination of different critic networks. This functions as a plug-and-play module within any cost-based planner, allowing a motion planner to leverage multiple critic networks as cost calculators simultaneously to pursue multiple planning goals. The only consideration is to assign appropriate weights to balance the trade-offs among them.

In the inference phase, we can flexibly combine the trained value networks. Additionally, we can incorporate supplementary costs related to goal orientation, safety, and efficiency. This integration results in a comprehensive and practical motion planner with enhanced explainability. Leveraging the proposed rule book, the inference model can be constructed with the following cost function:

$$C(\tau_i) = w_1 V_{R_{G1}} + w_2 V_{R_{I6}} + w_3 V_{R_{I3}} + \sum_i w_i C_i, \quad (4)$$

where $w_1 > w_2 > w_3$

Here, V represents the output of the trained value function, and C_i denotes any additional cost function.

IV. EXPERIMENTS

This chapter details our experimental investigation, spanning the foundational setup, implementation details, and a comparative analysis of our modified reinforcement learning (RL) approach against a baseline model. We leverage the highD dataset for evaluation. All experiments were conducted on a computing platform equipped with 12 CPUs, an Nvidia RTX 2060 GPU, and 30 GB of RAM. The training process was organized into three distinct phases, each targeting a specific traffic rule and comprising 20,000 steps.

A. Dataset

Our study employs the highD dataset [9], a comprehensive collection of naturalistic vehicle trajectories captured via drone-based aerial observation on German highways. It encompasses 1,255 traffic scenarios, each lasting 40–50 seconds and recorded at 25 Hz (0.04 s intervals) over 1,000 timesteps, presented in Bird’s Eye View (BEV) format. This mid-level representation provides detailed trajectory data, including vehicle specifications, dimensions, and maneuver patterns.

To adapt the dataset for our framework, we utilized the CommonRoad-Dataset Converter [18] to transform highD data into the CommonRoad format. During conversion, we adjusted the temporal resolution to 0.1 s intervals, optimizing the data structure for our learning algorithm while retaining sufficient granularity for precise trajectory analysis.

B. Experimental Setup

For the experiment, we selected 100 scenarios from the highD dataset. Given that no *no overtaking* signs are present in the original data, we manually inserted one into each scenario, randomly positioned between 100m and 350m along the longitudinal axis, to simulate a variety of situations.

TABLE III
ENVIRONMENT, MODEL AND TRAINING HYPERPARAMETERS

Parameter	Value
<i>Environment</i>	
Interval (s)	0.1
Ego vehicle start state (l_s, v_s)	150 m to 350 m from the goal, 15 m/s
Minimum Distance to Vehicles (m)	3
<i>Model</i>	
V2V graph construction	3-nearest neighbor $\forall \ \Delta p_{vw}\ _2 < 50$
GNN message passing layers (K)	3
Aggregation, activation functions	$\max(\cdot)$, $\tanh(\cdot)$
Feature dimensions ($ \mathbf{h}_v^{k>0} , \mathbf{z}_t $)	80, 80
GNN ego node-feature embedder	$MLP(\mathbf{h}_{ego} + f_{ego,LT} , \mathbf{z}_t)$
RL Actor-critic networks (π, V)	Each $MLP(256, 128, 64)$
<i>Motion Planner</i>	
Replanning Frequency (Hz)	2
Planning Horizon (s)	2
Sampling levels	2
Mode	Velocity Keeping
<i>Learning</i>	
Rollout steps	256
Discount factor (γ)	0.99
<i>Training</i>	
Optimizer	Adam
Learning rate	5×10^{-4}
Weight decay	10^{-3}
Number of epochs	8
Batch size	32

The comprehensive hyperparameters for the environment, model, and training are presented in Table III.

The experimental environment is designed with specific spatial configurations to ensure effective training scenarios. Each scenario includes a goal region randomly positioned 10 m to 50 m before the road’s terminus. The ego vehicle is initialized 150 m to 350 m from the goal, with an initial velocity of 15 m/s and a minimum clearance of 3 m from surrounding obstacles. This minimum distance allows the ego vehicle to spawn in challenging positions, enabling exploration of complex states.

At each training iteration, 256-step rollouts are collected and the return is computed using a discount factor of 0.99. This high value emphasizes the avoidance of long-term rule violations, prioritizing sustained reward accumulation over short-term gains.

Exploration is guided by the CommonRoad Reactive Planner [21], which operates with a replanning interval of 0.5 s and generates a set of trajectories spanning 20 timesteps (i.e., a 2 s horizon).

After each rollout step, the critic network is updated using collected states and rewards derived from the robustness of the rules with hyperparameters defined in Table III. The reactive planner’s cost function integrates these updated value estimates from the critic network, enabling continuous interaction with the environment through on-policy learning.

C. Rewards Design

We implement an independent training phase for each traffic rule, employing rule-specific robustness measures as reward signals with the same features, agent, and model. This separation facilitates focused learning of individual rule characteristics, minimizing cross-interference and eliminating

TABLE IV
REWARD COMPUTER FOR REINFORCEMENT LEARNING

Reward computer	Weight
<i>Phase 1</i>	
I2RobustnessRewardComputer	10
TrajectoryProgressionRewardComputer	8
<i>Phase 2</i>	
I6RobustnessRewardComputer	10
TrajectoryProgressionRewardComputer	8
<i>Phase 3</i>	
G1RobustnessRewardComputer	10
TrajectoryProgressionRewardComputer	8

the need to define and tune weights prior to training, thereby significantly streamlining the process.

Despite robustness-based rewards, we identified a challenge due to the absence of a termination reward. Without a positive reward for reaching the destination, and with a sparse or zero reward function throughout an episode, the cumulative future reward (i.e., the return) diminishes as the ego vehicle approaches the goal. This reduction occurs because fewer remaining steps limit opportunities to accumulate rewards, resulting in a counterintuitive decrease in the state-value function $V(s)$ near the destination—contrary to the expectation that states closer to the goal should have higher value due to their desirability. To address this, we introduce a *TrajectoryProgressionRewardComputer*, which provides positive rewards for advancing toward the goal, ensuring that the agent learns a policy that efficiently prioritizes its achievement.

The reward mechanism encourages progression toward the goal by rewarding both the extent and the rate of advancement. As the vehicle progresses, the arc length increases, contributing positively to the reward through the term $(1 - \text{dynamic_weight}) \times \text{arclength}$; even if progress slows near the goal, this term grows as the arc length approaches its maximum (e.g. 1 if normalized), reinforcing forward movement. Additionally, the $\Delta\text{arclength}$ term rewards the rate of progression, incentivizing the agent to move swiftly along the path when $\text{dynamic_weight} > 0$, whereas stalling (i.e., $\Delta\text{arclength} = 0$) yields a reward based solely on the static arc length, typically lower than that of continued advancement.

D. Benchmarking

To assess our approach, we established a non-learning baseline motion planner, employing the same reactive planner parameters as our method but incorporating traffic rule robustness costs directly. This baseline evaluates the trajectories by explicitly integrating compliance measures. For comparison, we defined a baseline cost function that substitutes learned value predictions with immediate rule evaluations via online robustness monitoring, which fundamentally differs from our learning-based approach, as it is limited to evaluating the immediate planning horizon. Consequently, it lacks the predictive capacity to foresee and mitigate rule violations beyond the current window, a limitation that our method overcomes through RL-driven foresight.

E. Evaluation

We use the explained variance metric and the episode reward mean metric to monitor and evaluate training.

1) *Explained Variance*: The explained variance measures how well the critic value function $V_\phi(s)$ predicts the actual returns (cumulative rewards) observed during training. It is defined as:

$$\text{Explained Variance} = 1 - \frac{\text{Var}(G_t - V_\phi(s_t))}{\text{Var}(G_t)} \quad (5)$$

where G_t is the true return (discounted sum of rewards from timestep t), $V_\phi(s_t)$ is the predicted value, and Var denotes variance. A value close to 1 indicates that the critic accurately captures the variability in returns, while a value close to 0 or negative suggests poor prediction.

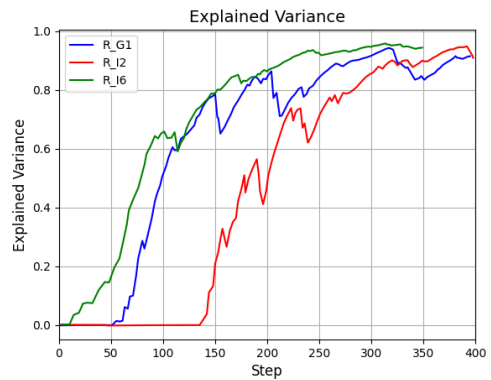


Fig. 3. Explained Variance

In Figure 3, the explained variance graph illustrates distinct learning dynamics for the traffic rules over 400 training steps. Specifically, R_{G1} demonstrates a steady increase, rising from 0.0 to approximately 0.9. This consistent ascent is particularly pronounced up to step 200, after which it stabilizes with minor fluctuations, reflecting the model’s progressively improving ability to predict returns. In contrast, R_{J2} exhibits greater volatility, characterized by notable peaks and troughs, while R_{J6} shows a slower, more gradual increase. The steady progress of R_{G1} indicates that the model effectively enhances its capacity to ensure long-term compliance with the safe distance rule, aligning with our evaluation objectives. Additionally, R_{I6} emerges as the easiest rule to learn, as it involves no vehicle-to-vehicle interactions, whereas R_{I2} proves the most challenging due to the extensive vehicle interactions it requires the model to capture.

2) *Episode Reward Mean*: The episode reward mean is the average total reward collected over an episode, a complete driving scenario from start to finish. For our setup, this likely reflects the cumulative robustness or compliance with traffic rules like R_{G1} , averaged across multiple episodes:

$$\text{Episode Reward Mean} = \frac{1}{N} \sum_{e=1}^N \sum_{t=0}^{T_e} r_t^e \quad (6)$$

where N is the number of episodes, T_e is the length of episode e , and r_t^e is the reward in time step t in episode e . This

metric evaluates the policy’s overall performance. A higher mean reward suggests that the ego vehicle is consistently achieving better outcomes.

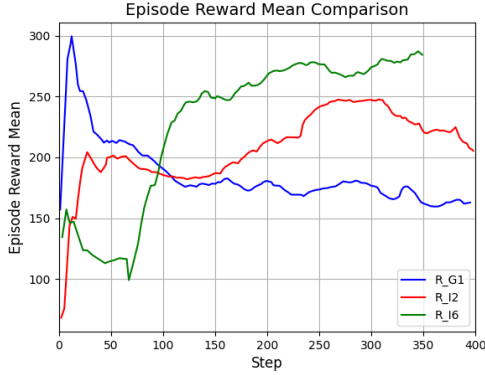


Fig. 4. Episode Reward mean

The *Episode Reward Mean Comparison* graph evaluates three configurations over 400 steps, with rewards ranging from 0 to 300. The blue line (R_{GI_1}) starts at ~ 300 but drops to ~ 150 by step 50, stabilizing thereafter, possibly due to early overfitting. The red line (R_{GI_2}) begins at ~ 50 , peaks at ~ 200 , and fluctuates between 150-250, indicating inconsistent performance. The green line (R_{I6}) starts near 0 and rises steadily to ~ 300 by step 400, surpassing the others with a robust upward trend. This suggests that R_{I6} achieves the highest long-term reward, reflecting better adaptability and learning efficiency.

3) *Performance of R_{I6} Predictive Model*: Our primary focus is on the custom rule R_{I6} , for which we compare the trained value network with the baseline model within the same scenario, featuring a *no overtaking* sign positioned at 300m along the longitudinal axis. We generate heatmaps using a grid-segmented representation of the road, evaluating the approximated state-value and R_{I6} rule robustness for both models. As depicted in Figure 5, a yellow grid indicates higher values, while a purple grid signifies lower values. The figure presents a comparative analysis of the trained value network and the baseline model, utilizing heatmaps overlaid on the road grid to assess the approximated state-value (top heatmap) and R_{I6} rule robustness (bottom heatmap). The color gradient spans from purple (low values) to yellow (high values), with blue vehicles marking the ego vehicle’s positions and gray dashed lines indicating lane markings or potential trajectories.

Baseline Model: The bottom heatmap displays a sharp yellow-to-purple transition between 250m and 300m, attributable to the traffic sign detection range being set at 50 m. This transition forms a rectangular shape, as the model increasingly avoids leftward positions as it approaches the sign. This suggests that the baseline model relies heavily on immediate rule evaluation, with limited foresight into the *no overtaking* constraint.

Trained Value Network: The top heatmap exhibits a smooth transition from yellow to purple, approximately aligning with the baseline model. However, the initial value change begins earlier, around 230m, compared to the 250m detection range,

the range increased from 50m to around 70m, indicating an awareness of long-term rule violation risks. Notably, the heatmap adopts a trapezoidal shape, with the value in the left lane decreasing earlier than in the right lane. Leveraging the predictive model, the lateral position of the ego vehicle influences the timing of lane-changing maneuvers: a vehicle positioned farther to the left can initiate a rightward lane change earlier, whereas a vehicle already near the right lane may delay the maneuver without violating the rule. This behavior aligns with human intuition and enhances safety and efficiency, as it enables proactive adjustments tailored to the vehicle’s spatial context.

The alignment between the robustness and state-value heatmaps of both models reinforces that rule robustness directly shapes the value function. However, the trained model’s smoother transitions suggest superior integration of long-term planning.

4) *Performance of R_{GI} Predictive Model*: The robustness of the value network output for rule R_{GI} is illustrated in Figure 6, where the speed of the ego vehicle is set to 25 m/s to simulate a vehicle approaching rapidly. In the bottom heatmap depicting the robustness of the rule, the positions directly behind each vehicle exhibit lower robustness, with the area behind the vehicle in the left lane showing the lowest values. Robustness remains higher in the right lane, particularly at greater lateral distances from vehicles, suggesting that maintaining an offset reduces collision risk.

The upper heatmap, which represents the output of the value network, shows broader and larger unsafe regions behind vehicles compared to the robustness heatmap. For example, for the vehicle at (150 m, -31 m), the robustness heatmap indicates low values only in the grids directly behind it. In contrast, the output of the value network increases in adjacent lateral positions as the ego vehicle approaches, reflecting consideration of possible lane changes. This adjustment allows the model to account for dynamic scenarios, such as sudden maneuvers by other vehicles, and supports a more conservative policy to prevent R_{GI} violations. The value network’s ability to incorporate longer-term predictions distinguishes it from the baseline model, enhancing its effectiveness in managing variable traffic conditions.

5) *Performance of R_{I2} Predictive Model*: In Figure 7, the speed of the ego vehicle is set to 25 m/s. The robustness heatmap indicates that the positive robustness is limited to the leftmost lane and specific grids in the middle lane where gaps between vehicles occur. This pattern highlights that 25 m/s exceeds the speed of most surrounding vehicles, restricting rule-compliant positions to areas where the ego vehicle avoids direct adjacency to slower vehicles on its left. In the value heatmap, which represents the model’s evaluation of long-term compliance and reward potential, the right lane consistently exhibits low values, aligning with the robustness findings. In contrast, the left lane shows higher values in the first half of the road compared to the second half. This variation is attributed to a slower moving vehicle at coordinates (75, -21), increasing the risk of violating the rule R_{I2} when the ego vehicle travels along it. Such insights could enable the vehicle to make more informed and sensitive decisions. However, the prediction of

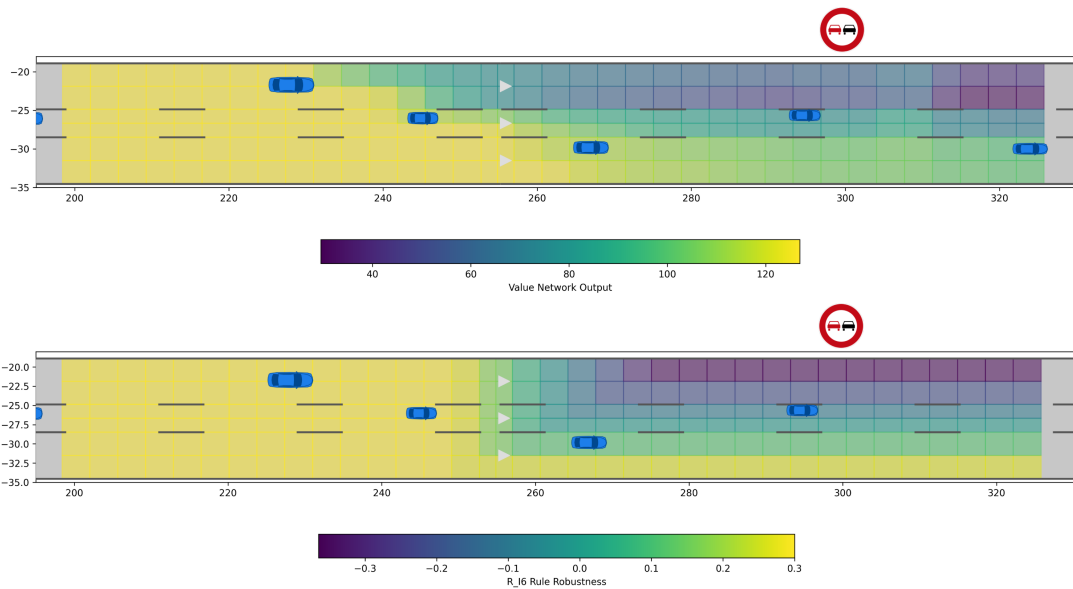


Fig. 5. Heatmap comparison of state-value and rule robustness for R_{I6}

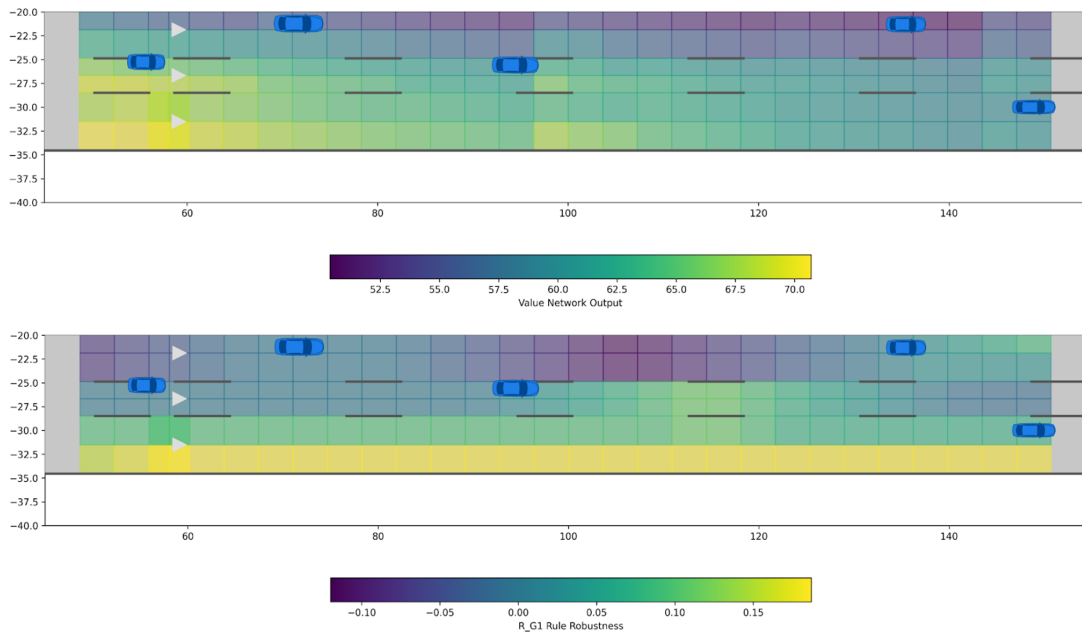


Fig. 6. Heatmap comparison of state-value and rule robustness for R_{G1}

values shows significant volatility, consistent with the analysis of “Explained Variance”, underscoring the learning challenges associated with R_{I2} . This volatility suggests that additional training data and extended learning periods are essential to improve the stability and predictive accuracy of the model.

F. Discussion

This experiment demonstrates the model’s capability to predict long-term violations of traffic rules within the highD dataset scenarios. The proposed RL approach facilitates safer and more efficient trajectory planning by enabling the system to anticipate potential rule violations and adjust maneuvers proactively, reducing the likelihood of entering states that lead

to unavoidable violations. For rules R_{I6} and R_{G1} , which involve constraints independent of direct vehicle-to-vehicle interactions or focus on maintaining safe distances, the method exhibits strong performance, as evidenced by the smoother transitions in the value network outputs and the expanded safety regions in the heatmaps.

However, the model shows reduced robustness for rules involving complex vehicle interactions, such as R_{I2} , which requires maintaining appropriate speeds relative to surrounding vehicles. This limitation is reflected in the volatility observed in the explained variance metric and the inconsistent value predictions in the heatmap analysis. The challenge arises from the intricate dynamics of vehicle interactions, which demand

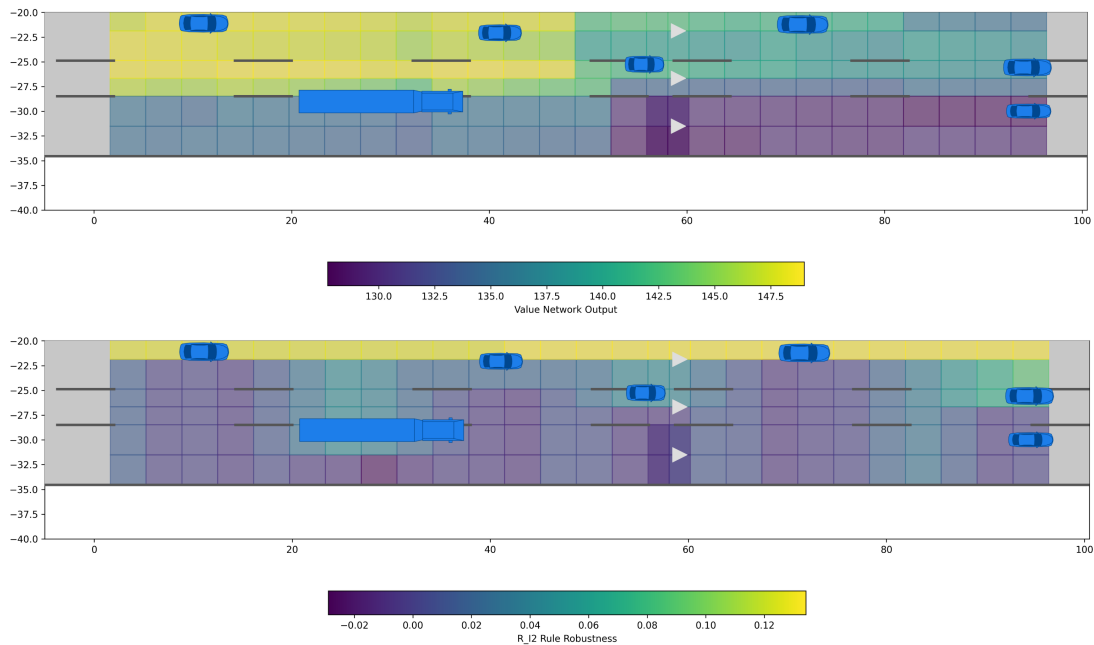


Fig. 7. Heatmap comparison of state-value and rule robustness for R_{I2}

a more detailed understanding of relative positions, speeds, and potential maneuvers. Addressing this issue may require enhancements such as increasing the volume of training data, extending the training duration, and incorporating additional features, such as relative velocity or lane-changing probabilities, to better capture the interaction dynamics. Furthermore, adopting a more advanced scenario extraction model, such as a Heterogeneous Graph Neural Network, could enhance the model’s ability to represent and manage complex traffic interactions by accounting for diverse vehicle types and their interconnected behaviors.

V. CONCLUSION

This thesis introduces a hybrid framework aimed at enhancing traffic rule compliance in autonomous driving systems. The approach addresses the limitation of short prediction horizons in traditional planning methods by integrating an actor-critic deep reinforcement learning (DRL) algorithm with a cost-based motion planner. This combination enables improved predictive compliance with traffic rules, particularly in complex highway scenarios on German interstate roads, as evaluated using the highD dataset. A Graph Neural Network (GNN) is utilized to construct a detailed state representation, allowing the critic network to learn state-value functions that anticipate potential rule violations beyond the immediate planning horizon. Experiments conducted on the highD dataset demonstrate that this method achieves better performance compared to a non-learning baseline, as evidenced by smoother transitions in state-value and robustness heatmaps for specific traffic rules, such as R_{I6} and R_{G1} .

The proposed framework contributes to autonomous driving technology by developing a hierarchically structured rule book based on German traffic regulations and implementing a modular system compatible with cost-based motion planners.

This modular design ensures flexibility, allowing the system to be adapted to various planning architectures with minimal adjustments.

In summary, this thesis provides a robust and adaptable solution for predictive traffic rule compliance in autonomous driving. By combining learning-based prediction with planning, the hybrid approach enhances compliance with traffic rules and supports safer navigation in dynamic environments. The framework establishes a foundation for future research in autonomous vehicle technology, particularly in improving the handling of complex vehicle interactions. As autonomous driving continues to develop, such frameworks may contribute to the realization of fully autonomous, rule-compliant systems, potentially leading to safer and more efficient roadways.

REFERENCES

- [1] M. Burmann, R. Heß, K. Hühnermann, and J. Jahnke. *Straßenverkehrsrecht: Kommentar*. 2018.
- [2] A. Censi et al. Liability, ethics, and culture-aware behavior specification using rulebooks. In *2019 International Conference on Robotics and Automation (ICRA)*, pages 8536–8542, 2019.
- [3] Q. Gao, D. Hajinezhad, Y. Zhang, et al. Reduced variance deep reinforcement learning with temporal logic specifications. In *Proceedings of the 10th ACM/IEEE International Conference on Cyber-Physical Systems*, pages 237–248, 2019.
- [4] G. Gkarpounis, C. Vranis, N. Vretos, and P. Daras. Survey on graph neural networks. *IEEE Access*, 12:128816–128832, 2024.
- [5] L. Gressenbuch and M. Althoff. Predictive monitoring of traffic rules. In *2021 IEEE International Intelligent Transportation Systems Conference (ITSC)*, pages 915–922, 2021.
- [6] P. Hart and A. Knoll. Graph neural networks and reinforcement learning for behavior generation in semantic environments. *arXiv preprint arXiv:2006.12576*, 2020.
- [7] M. I. Jordan and T. M. Mitchell. Machine learning: Trends, perspectives, and prospects. *Science*, 349(6245):255–260, 2015.
- [8] R. Koymans. Specifying real-time properties with metric temporal logic. *Real-Time Syst.*, 2(4):255–299, 1990.

- [9] R. Krajewski, J. Bock, L. Kloeker, and L. Eckstein. The highD dataset: A drone dataset of naturalistic vehicle trajectories on german highways for validation of highly automated driving systems. In *2018 21st International Conference on Intelligent Transportation Systems (ITSC)*, pages 2118–2125, 2018.
- [10] S. Maierhofer, P. Moosbrugger, and M. Althoff. Formalization of intersection traffic rules in temporal logic. In *2022 IEEE Intelligent Vehicles Symposium (IV)*, pages 1135–1144, 2022.
- [11] S. Maierhofer, A.-K. Rettinger, E. C. Mayer, and M. Althoff. Formalization of interstate traffic rules in temporal logic. In *2020 IEEE Intelligent Vehicles Symposium (IV)*, pages 752–759, 2020.
- [12] O. Maler and D. Nickovic. Monitoring temporal properties of continuous signals. In Y. Lakhnech and S. Yovine, editors, *Formal Techniques, Modelling and Analysis of Timed and Fault-Tolerant Systems*, pages 152–166, 2004.
- [13] E. Meyer, M. Brenner, B. Zhang, M. Schickert, B. Musani, and M. Althoff. Geometric deep learning for autonomous driving: Unlocking the power of graph neural networks with CommonRoad-Geometric. *arXiv preprint arXiv:2302.01259*, 2023.
- [14] D. Nickovic and T. Yamaguchi. Rtamt: Online robustness monitors from stl. *arXiv preprint arXiv:2005.11827*, 2020.
- [15] L. F. Peiss, E. Wohlgemuth, F. Xue, E. Meyer, L. Gressenbuch, and M. Althoff. Graph-based autonomous driving with traffic-rule-enhanced curriculum learning. In *2023 IEEE International Conference on Intelligent Transportation Systems (ITSC)*, 2023.
- [16] J. Rong and N. Luan. Safe reinforcement learning with policy-guided planning for autonomous driving. In *2020 IEEE International Conference on Mechatronics and Automation (ICMA)*, pages 320–326. IEEE, 2020.
- [17] R. S. Sutton and A. G. Barto. *Reinforcement Learning: An Introduction*. A Bradford Book, Cambridge, MA, USA, 2018.
- [18] X. Wang et al. CommonRoad-Dataset-Converter: Tools for converting various datasets to CommonRoad format, 2024. Software Project at Technical University of Munich.
- [19] M. Werling, S. Kammel, J. Ziegler, and L. Groell. Optimal trajectories for time-critical street scenarios using discretized terminal manifolds. *Int. J. Robot. Res.*, 31:346–359, 2012.
- [20] M. Werling, J. Ziegler, S. Kammel, and S. Thrun. Optimal trajectory generation for dynamic street scenarios in a Frenét frame. pages 987–993, 2010.
- [21] Gerald Würsching. Commonroad/commonroad-reactive-planner, 8 2024. Accessed: December 08, 2024.